DOI: 10.1002/cmdc.201200303

MT_1-Selective Melatonin Receptor Ligands: Synthesis, Pharmacological Evaluation, and Molecular Dynamics Investigation of *N*-{[(3-*O*-Substituted)anilino]alkyl}amides

Silvia Rivara,[a] Daniele Pala,[a] Alessio Lodola,[a] Marco Mor,[a] Valeria Lucini,[b] Silvana Dugnani,[b] Francesco Scaglione,[b] Annalida Bedini,[c] Simone Lucarini,[c] Giorgio Tarzia,[c] and Gilberto Spadoni*[c]

The design of compounds selective for the MT_1 melatonin receptor is still a challenging task owing to the limited knowledge of the structural features conferring selectivity for the MT_1 subtype, and only few selective compounds have been reported so far. *N*-(Anilinoalkyl)amides are a versatile class of melatonin receptor ligands that include nonselective MT_1/MT_2 agonists and MT_2-selective antagonists. We synthesized a new series of *N*-(anilinoalkyl)amides bearing 3-arylalkyloxy or 3-alkyloxy substituents at the aniline ring, looking for new potent and MT_1-selective ligands. To evaluate the effect of substituent size and shape on binding affinity and intrinsic activity, both flexible and conformationally constrained derivatives were prepared. The phenylbutyloxy substituent gave the best result, providing the partial agonist **4a**, which was endowed with high MT_1 binding affinity ($pK_i = 8.93$) and 78-fold selectivity for the MT_1 receptor. To investigate the molecular basis for agonist recognition, and to explain the role of the 3-arylalkyloxy substituent, we built a homology model of the MT_1 receptor based on the β_2 adrenergic receptor crystal structure in its activated state. A binding mode for MT_1 agonists is proposed, as well as a hypothesis regarding the receptor structural features responsible for MT_1 selectivity of compounds with lipophilic arylalkyloxy substituents.

Introduction

Melatonin (*N*-acetyl-5-methoxytryptamine (**1**), Figure 1) is a neurohormone primarily secreted by the pineal gland at night in all species.[1] Melatonin has been claimed to have an effect in almost all of the main physiological functions of the body,[2] particularly in circadian rhythms and sleep regulation,[3] control of mood and behavior,[4,5] neuroimmunomodulation,[6] blood pressure control,[7] and pain perception.[8] Moreover, anti-inflammatory,[9] antioxidant,[10] neuroprotectant,[11] and antitumor[12,13] activities have been ascribed to melatonin. Recently, the melatonin signaling pathway has been implicated in the events leading to the development of type 2 diabetes.[14,15] Although the endogenous role of melatonin and the mechanisms by which it regulates the physiology of mammalian and non-mammalian species have not been fully elucidated, three therapeutic agents targeting the melatonin membrane receptors (Circadin,[16] Rozerem,[17] and Valdoxan[18]) are already in use, and melatonin receptor agonists are now appearing as new promising therapeutic options in the treatment of circadian rhythm sleep disorders and depression.[19,20] Melatonin interacts with high-affinity G protein-coupled receptors (GPCRs), two of which, MT_1 and MT_2, have been found in mammals, including humans, and subsequently cloned.[21] Both MT_1 and MT_2 receptors exhibit sub-nanomolar binding affinity for melatonin and are negatively coupled to adenylate cyclase, although they can also interact with other intracellular signaling pathways.[22] A third melatonin receptor subtype, termed Mel_{1c}, has been cloned from *Xenopus laevis*, chicken, and zebrafish, but it is not expressed in mammals.[23] In addition to these high-affinity GPCRs, a distinct binding site, termed MT_3 and displaying lower affinity for melatonin ($K_i = 10$–60 nM), was purified and characterized as the hamster homologue of the human enzyme quinone reductase 2.[24] In mammals, melatonin receptors are mainly expressed in the brain, with considerable variation in the location and density of expression among species and also in some peripheral tissues.[25,26] The differential role of MT_1 and MT_2 subtypes has been only partially elucidated. Experimental evidence supports that activation of MT_1 receptors in mice inhibits neuronal firing within the SCN,[27] inhibits prolactin secretion in photoperiodic species,[28] modulates visual function in mouse retina,[29] and induces vasoconstriction of rat caudal arteries.[30] On the other hand, activation

[a] Prof. S. Rivara, Dr. D. Pala, Dr. A. Lodola, Prof. M. Mor
Dipartimento di Farmacia, Università degli Studi di Parma
V.le G. P. Usberti 27A, 43124 Parma (Italy)

[b] Dr. V. Lucini, Dr. S. Dugnani, Prof. F. Scaglione
Dipartimento di Farmacologia, Chemioterapia e Tossicologia Medica
Università degli Studi di Milano
Via Vanvitelli 32, 20129 Milano (Italy)

[c] Dr. A. Bedini, Dr. S. Lucarini, Prof. G. Tarzia, Prof. G. Spadoni
Dipartimento di Scienze Biomolecolari
Università degli Studi di Urbino "Carlo Bo"
Piazza Rinascimento 6, 61029 Urbino (Italy)
E-mail: gilberto.spadoni@uniurb.it

Supporting information for this article is available on the WWW under http://dx.doi.org/10.1002/cmdc.201200303.

© 2012 Wiley-VCH Verlag GmbH & Co. KGaA, Weinheim

of MT_2 receptors induces vasodilation,[31] enhances immune function,[32] inhibits dopamine release in rabbit retina,[33] produces a phase shift in circadian rhythms,[34] and promotes non-rapid eye movement sleep in rats.[35]

Studies aimed at characterizing the pathophysiological role of melatonin should take advantage of the availability of compounds selective for either the MT_1 or MT_2 receptor subtype. Whereas numerous MT_2-selective ligands have been described (for reviews, see references [36], [37], and [38]), the literature only reports a few examples of MT_1-selective compounds. MT_1-selective ligands (Figure 1) comprise different series of dimeric compounds. Homo- and heterodimers of the agomelatine scaffold exhibited nanomolar binding affinities for MT_1.[39,40] Dimers based on the indole,[41] 4-azaindole,[42] or aniline[43] skeleton were also reported, but they exhibited weaker affinity and MT_1-selectivity than the parent naphthalene dimers. Of the dimeric compounds, a three methylene linker conferred the highest MT_1 selectivity.[39,43] Compounds with sub-nanomolar affinity but modest selectivity for the MT_1 subtype were obtained introducing a 4-phenylbutyl substituent in position 2 of the benzoxazole or benzofuran ring in different series of melatoninergic ligands.[44] The presence of a linear hexyloxy chain in position 6 of chromane derivative S25567 conferred some selectivity for the MT_1 receptor.[45] Recently, a series of melatonin indole derivatives bearing different 5-arylalkyloxy substituents has been described, with some compounds having approximate 10-fold selectivity for the MT_1 receptor when a phenyl ring is connected to the oxygen atom in position 5 with a three methylene or a three-methyl-oxy linker.[46] MT_1-selective ligands reported so far share a common structural feature, that is, a bulky lipophilic substituent connected to the oxygen atom in position 5 of melatonin, or in the topologically equivalent position in ligands with different scaffolds. However, the identification and fine-tuning of suitable steric and physicochemical properties of the substituents able to confer MT_1 subtype selectivity are still a challenge, as only sparse information is available, and no conclusive structure–activity relationships (SARs) have been reported. The symmetrical structure of dimeric compounds previously suggested that the two outer units of melatonin bioisosteres could bind two orthosteric binding sites in two units of receptor homodimers,[39] even though longer spacers are reported to be required by bivalent ligands.[47] On the other hand, one of the two outer portions could be replaced by a simple lipophilic group at no cost of MT_1 affinity,[39] and allosteric binding sites have recently been characterized in the extracellular regions of different GPCRs. This prompts an alternative hypothesis: that lipophilic groups emerging from the aromatic portion of melatonin receptor ligands would be accommodated in a channel pointing toward the extracellular loops. Further pursuit of this hypothesis requires that isosteric replacement of one moiety in dimeric ligands by non-melatonin-like groups be conserved in different classes of melatonin receptor ligands with some MT_1 selectivity, and that a channel exists that can accommodate such groups within the structure of the MT_1 receptor, as far as this can be postulated from the known three-dimensional structures of crystallized GPCRs.

We recently discovered a class of high affinity melatonin receptor ligands having a *N*-(anilinoethyl)amide scaffold. This class was very versatile, as it could be properly functionalized to provide non-selective MT_1/MT_2 agonists or MT_2-selective partial agonists and antagonists.[48] Moreover, metabolically protected derivatives could be obtained which maintained the same receptor profile as the parent compounds.[49] We report here the synthesis and pharmacological characterization of new *N*-(3-*O*-substituted-anilinoalkyl)amides (**4a–n**) in which lipophilic substituents of different size and shape were introduced at the oxygen atom of the aniline core. We investigated arylalkyl and alkyl substituents looking for optimal chain length. We also prepared some conformationally constrained derivatives with the aim of defining the conformational preference of the flexible alkyl chain. Moreover, a three-dimensional (3D) model of the active form of the MT_1 receptor was built by homology modeling, and a binding scheme for agonist compounds is hypothesized. Based on the different amino acid composition of MT_1 and MT_2 receptors, an explanation for the MT_1 selectivity of compounds carrying arylalkyloxy substituents is proposed.

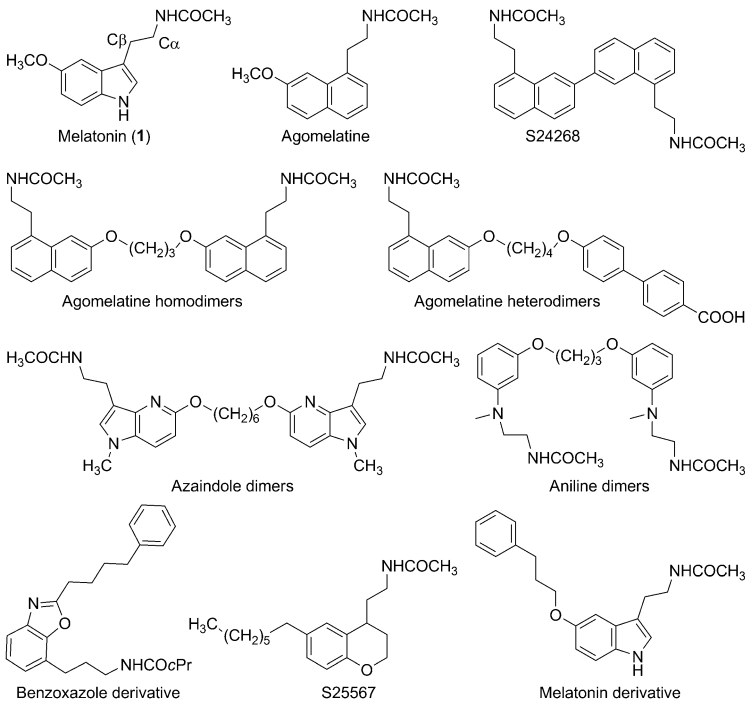

Figure 1. Structures of melatonin, agomelatine, and representative MT_1-selective ligands.

Results and Discussion

Chemistry

The new melatonin receptor ligands **4a–n** were synthesized as described in Scheme 1. Phenol derivatives

 © 2012 Wiley-VCH Verlag GmbH & Co. KGaA, Weinheim

These are not the final page numbers!

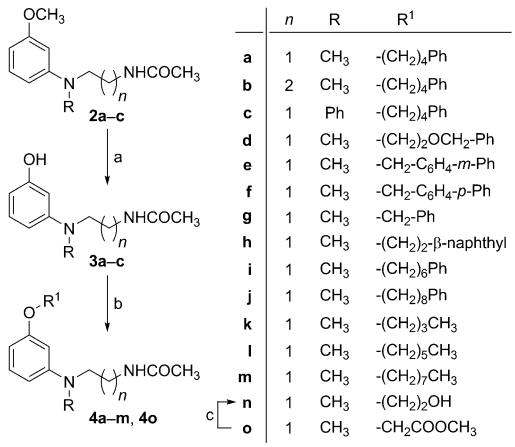

Scheme 1. *Reagents and conditions*: a) BBr_3, CH_2Cl_2, RT, 18 h; b) NaH, R^1X, DMF, RT, 8–16 h (or 2-(2-bromoethyl)naphthalene, K_2CO_3, CH_3CN, RT, 16 h for **4h**); c) $LiAlH_4$, THF, 0 °C, 1 h.

3a–c were obtained by ether cleavage of the corresponding methoxy derivatives **2a–c**[48] using boron tribromide. Subsequent O-alkylation of phenols **3a–c** with a suitable alkyl- or arylalkylhalide in the presence of a base (NaH, or K_2CO_3 for **4h**) afforded the O-alkylated compounds **4a–m** and **4o**. Hydroxyethoxy derivative **4n** was prepared by $LiAlH_4$ reduction of the corresponding ester **4o**.

Structure–activity relationships

Binding affinities and intrinsic activities at the human MT_1 and MT_2 receptors of the newly synthesized *N*-(anilinoethyl)acetamides with 3-alkyloxy- or 3-arylalkyloxy substituents (**4a–n**) were assessed as described in the Experimental Section. Results are reported in Table 1, along with data for a number of reference compounds. A total of 12 new compounds (**4a** and **4d–n**) were examined to investigate the effect of length, size, and shape of the aniline-3-O-substituent on MT_1/MT_2 subtype selectivity. Combination with arylation of the aniline nitrogen (**4c**) and lengthening of the ethyl spacer (**4b**) were also evaluated. Replacement of the ether methyl group of non-selective agonist **2a** with a phenylbutyl substituent (**4a**) gave the expected favorable effect on MT_1/MT_2 selectivity. Phenylbutyloxy derivative **4a** showed high binding affinity for MT_1 receptors ($pK_i = 8.93$) and considerably lower affinity for MT_2 receptors ($pK_i = 7.04$), thus leading to a MT_1/MT_2 selectivity ratio of 78. Compound **4a** is one of the most MT_1-selective compounds reported in the literature, although it could not reach the 100-200-fold selectivity measured for some agomelatine homodimers;[39] this high selectivity, however, could not be reproduced by other authors, who observed threefold selectivity for the reference derivative.[46] Interestingly, introduction of the phenylbutyloxy substituent on the melatonin indole ring did not provide any selectivity,[45] suggesting that the effect of specific lipophilic substituents may be class-dependent. The presence

Table 1. Binding affinity (pK_i) and intrinsic activity (IA_r) of *N*-{[(3-*O*-substituted)anilino]alkyl}amide derivatives at human MT_1 and MT_2 melatonin receptors stably expressed in NIH3T3 cells.

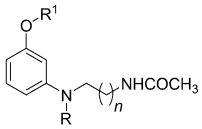

Compd	*n*	R	R^1	hMT_1		hMT_2	
				pK_i[a]	IA_r[b]	pK_i[a]	IA_r[b]
melatonin (**1**)				9.39 ± 0.08	1.00 ± 0.01	9.47 ± 0.13	1.00 ± 0.02
2a[47]	1	CH_3	CH_3	9.09	0.95	9.19	1.06
4a	1	CH_3	$(CH_2)_4Ph$	8.93 ± 0.17	0.68 ± 0.09	7.04 ± 0.10	0.61 ± 0.05
4b	2	CH_3	$(CH_2)_4Ph$	8.07 ± 0.23	0.23 ± 0.04	6.22 ± 0.12	0.28 ± 0.06
4c	1	Ph	$(CH_2)_4Ph$	7.45 ± 0.01	0.12 ± 0.02	6.48 ± 0.29	0.01 ± 0.01
4d	1	CH_3	$(CH_2)_2$-O-CH_2Ph	8.60 ± 0.01	0.81 ± 0.05	7.63 ± 0.03	0.98 ± 0.05
4e	1	CH_3	CH_2-C_6H_4-*m*-Ph	7.42 ± 0.27	−0.07 ± 0.03	6.42 ± 0.10	0.08 ± 0.03
4f	1	CH_3	CH_2-C_6H_4-*p*-Ph	7.42 ± 0.14	0.47 ± 0.02	6.53 ± 0.21	0.79 ± 0.27
4g	1	CH_3	CH_2Ph	6.98 ± 0.07	0.15 ± 0.05	6.74 ± 0.18	0.54 ± 0.05
4h	1	CH_3	$(CH_2)_2$-β-naphthyl	7.32 ± 0.16	0.41 ± 0.03	6.55 ± 0.17	0.66 ± 0.05
4i	1	CH_3	$(CH_2)_6Ph$	7.81 ± 0.23	0.61 ± 0.02	6.56 ± 0.10	0.23 ± 0.03
4j	1	CH_3	$(CH_2)_8Ph$	7.60 ± 0.17	0.60 ± 0.02	6.71 ± 0.04	0.44 ± 0.10
4k	1	CH_3	$(CH_2)_3CH_3$	8.56 ± 0.11	0.73 ± 0.01	8.49 ± 0.47	0.80 ± 0.07
4l	1	CH_3	$(CH_2)_5CH_3$	9.01 ± 0.13	0.80 ± 0.01	8.62 ± 0.19	1.05 ± 0.01
4m	1	CH_3	$(CH_2)_7CH_3$	7.14 ± 0.05	0.61 ± 0.07	6.54 ± 0.05	0.31 ± 0.02
4n	1	CH_3	$(CH_2)_2OH$	7.08 ± 0.12	0.42 ± 0.14	6.44 ± 0.26	0.11 ± 0.07
5[47]	2	CH_3	CH_3	9.08	0.87	8.70	1.07
6[47]	1	Ph	CH_3	8.38	0.79	10.18	0.61

[a] pK_i values are calculated from IC_{50} values that were obtained from competition curves by the method of Cheng and Prusoff,[53] and are the mean ± SEM of at least three determinations performed in duplicate. [b] Relative intrinsic activity values were obtained by dividing the maximum analogue-induced G protein activation by that of melatonin. Data represent the mean ± SEM of at least three determinations performed in duplicate.

 © 2012 Wiley-VCH Verlag GmbH & Co. KGaA, Weinheim

of the phenylbutyl chain also affected intrinsic activity, as compound **4a** behaved as a partial agonist at both receptor subtypes. Similarly, MT_1-selective agomelatine homo- and heterodimers showed a decreased ability to activate melatonin receptors.[40,41]

Elongation of the ethylamido side chain in **4a** by one methylene group (**4b**) led to a slight decrease in MT_1 and MT_2 binding affinities, maintaining the same selectivity ratio (MT_2/MT_1 K_i $=71$). Relative to its methoxy analogue **5**, compound **4b** showed enhanced MT_1 selectivity. The presence of a phenyl ring on the aniline nitrogen (**4c**) had a negative effect on MT_1 binding affinity without significantly affecting potency at MT_2 receptors and resulting in a loss in MT_1 selectivity (MT_2/MT_1 K_i ≈ 10). Indeed, an *N*-phenyl substituent is a structural element conferring selectivity for the MT_2 receptor, as can be seen for partial agonist **6**.[48] It has been proposed that the phenyl substituent can occupy a region of the melatonin receptors that is larger and more accessible in the MT_2 receptor than in the MT_1, thus leading to the observed MT_2 selectivity.[50] Combination of two substituents conferring opposite subtype selectivity provided low binding affinity at both receptor subtypes (**4c**). Replacement of one methylene group of the butyl chain with an oxygen atom in compound **4d** led to a modest decrease in MT_1 binding affinity and to an increased affinity for the MT_2 receptor, resulting in a loss of selectivity (MT_2/MT_1 K_i ≈ 10). The presence of an additional ether linkage influenced intrinsic activity, converting a partial agonist (**4a**) into a full agonist (**4d**). To investigate the preferred conformation of the phenylbutyloxy chain, we replaced the flexible substituent with either a *meta*- (**4e**) or *para*- (**4f**) biphenylmethyloxy group. Unfortunately, these bulkier aromatic ring systems resulted in a great loss in binding affinity at both receptor subtypes and to antagonist behavior for **4e**. The decreased affinity could be ascribed to the presence of a proximal phenyl ring. In fact, the MT_1 binding affinity of benzyloxy derivative **4g** was very modest, and the second phenyl ring in **4e** and **4f** provided only a limited increase in binding affinity, irrespective of the *meta* or *para* substitution. The 5-benzyloxy substituent showed a different behavior on the melatonin scaffold, being tolerated particularly at the MT_2 receptor and leading to some selectivity for this receptor subtype.[46,51] Rigidification of the arylalkyl side chain in a more distal position in compound **4h**, carrying a β-naphthylethyloxy substituent, did not lead to any improvement in binding affinity and subtype selectivity relative to the biphenyl derivatives. Elongation of the alkyl chain of the phenylalkyloxy substituent to six (**4i**) or eight (**4j**) methylene units provided compounds with MT_1 binding affinity lower than that of tetramethylene derivative **4a**, which is the most potent and MT_1-selective phenylalkyloxy derivative of the series. Removal of the terminal phenyl ring in alkyloxy derivatives **4k–l** mainly influenced subtype selectivity. While affinity for MT_1 receptors was retained, the smaller alkyl groups were better tolerated at the MT_2 receptor. Compound **4l**, with a hexyloxy substituent, is a potent nonselective melatonin receptor agonist. A further increase in alkyl chain length resulted in a considerable decrease in binding affinity at both receptors (**4m** versus **4l**). Finally, we investigated the effect of the 2-hydroxyethyloxy substituent on the *N*-anilinoethylamide structure. 5-HEAT (*N*-{2-[5-(2-hydroxyethoxy)-1*H*-indol-3-yl]ethyl}acetamide) is a functional MT_1-selective compound, having similar binding affinities for MT_1 and MT_2 receptors but showing MT_1 agonist and MT_2 antagonist behavior (relative intrinsic activities: $MT_1=0.92$, $MT_2=0.16$).[52] Compound **4n** had similar low MT_1 and MT_2 intrinsic activities and low binding affinities.

Molecular modeling

Recently, a number of experimentally determined 3D structures of agonist-bound GPCRs crystallized in their fully active state have been reported, such as those of rhodopsin and the β_2 adrenergic receptor. In addition to their importance in deciphering the receptor activation mechanism at a molecular level, these agonist-bound receptors represent valuable template structures for the building of novel homology models of class A GPCRs. We therefore started from these active receptor configurations to build a new MT_1 homology model with the aim of investigating the molecular basis of agonist recognition and MT_1 selectivity. Prediction of the 3D structure of melatonin receptors can be considered a challenging task, given the availability of structural templates showing only a limited percentage identity (<30% within the transmembrane (TM) domains) with the target sequences. A further element which makes melatonin receptor modeling even more challenging is the lack of well-characterized ligand–receptor contacts. Mutagenesis studies of melatonin receptors resulted in sparse information and did not provide a definite binding scheme.[21] Difficulty in the identification of the binding mode for melatonin could be due to its lipophilic character and to the receptor amino acid composition. Indeed, melatonin functional groups cannot undertake strong polar interactions, and melatonin receptors are non-aminergic GPCRs that lack the complex pattern of crucial amino acids that are known to anchor the polar substituents of endogenous amines (e.g., the conserved aspartic residue located on TM3). However, even if the modeling of melatonin receptors must cope with the high degree of uncertainty of available structural information, it could take advantage of the amount of ligand-based information available thus far, such as structure–activity relationships and pharmacophore models.

The crystal structure of the fully activated β_2 adrenergic receptor (PDB code: 3P0G)[54] was used for homology modeling of the MT_1 receptor (see Experimental Section), and induced-fit docking (IFD)[55] was applied to shape the putative binding site around the structure of 2-phenylmelatonin (2PhMLT); 2PhMLT was chosen because it is one of the most potent melatonin receptor agonists,[56] and its bulky structure was suitable to define and model the MT_1 binding site. 2PhMLT was rigidly docked, with the conformation of the ethylamide side chain and the methoxy group consistent with a previously developed pharmacophore model for melatoninergic agonists.[57] Indeed, introduction of this ligand-based information allowed us to focus only on those receptor–ligand complexes consistent with known SARs. Resulting MT_1 receptor–2PhMLT complexes were evaluated according to both their docking scores

 © 2012 Wiley-VCH Verlag GmbH & Co. KGaA, Weinheim

and to agreement with the indications provided by mutagenesis. Site-directed mutagenesis performed on the MT_1 receptor suggested that His 195$^{5.46}$ (superscripts refer to Ballesteros-Weinstein numbering[58]), located on TM5, is likely to be involved in the stabilization of the 5-methoxy group of melatonin, as its mutation led to a three- to eightfold decrease in binding affinity only for ligands carrying the 5-methoxy substituent.[59,60] A similar result was obtained by mutation of the corresponding histidine (His 208$^{5.46}$) on the MT_2 receptor.[61] Therefore, the best ranked MT_1 receptor–2PhMLT complex having a 5-methoxy group in proximity to His 195$^{5.46}$ was selected for further analysis. To evaluate the stability of the ligand–receptor interactions in the resulting binding pose, a molecular dynamics (MD) simulation was carried out in a solvated lipid bilayer for 50 ns. As shown in Figure 2, the root mean squared deviation (RMSD) calculated for TM alpha carbons reached a plateau after 15 ns of simulation, confirming the stability of the receptor 3D structure.

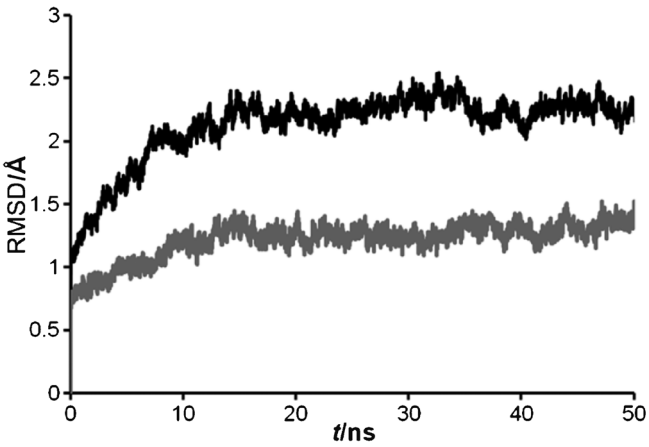

Figure 2. RMSD for the α-carbons of TM regions of the MT_1 receptor in complex with 2PhMLT (black) and **4a** (gray) during a 50 ns MD simulation.

Visual inspection of trajectories revealed that ligand–receptor interactions remained stable for the whole simulation, and 2PhMLT retained its initial conformation and orientation within the ligand binding site. 2PhMLT was accommodated into a binding site crevice between TM3, TM4, TM5, TM6, and TM7. The agonist molecule formed two hydrogen bond interactions between the amide oxygen and the hydroxy group of Tyr 285$^{7.43}$ and between the methoxy oxygen and the hydroxy group of Tyr 187$^{5.38}$ (Figure 3). No mutagenesis data on the MT_1 receptor are available for these two tyrosines. However, Tyr 298$^{7.43}$ in the MT_2 receptor, corresponding to MT_1 Tyr 285$^{7.43}$, was found to be crucial for agonist stabilization, as mutation of this residue to alanine completely abolished melatonin binding.[62] The involvement of position 5.38 in ligand binding has been extensively investigated in different class A GPCRs through mutagenesis studies, highlighting a key role of this amino acid in ligand stabilization. For example, the non-aminergic A_{2A} adenosine receptor mutation of Met 177$^{5.38}$, which directly interacts with the furan ring of the co-crystallized antagonist ZM241385,[63] resulted in an eightfold decrease in antagonist binding.[64] Site-directed mutagenesis performed on the V1a vasopressin receptor[65] and the α_{1B} adrenergic receptor[66] clearly highlighted the importance of the tyrosine residue at position 5.38 in agonist binding. The indole ring of 2PhMLT was sandwiched between Gly 108$^{3.33}$ and His 195$^{5.46}$, and the 2-phenyl ring was accommodated within an additional cavity formed by Trp 251$^{6.48}$, Leu 254$^{6.51}$, Asn 255$^{6.52}$, Tyr 281$^{7.39}$, and Ala 284$^{7.42}$; two edge-to-face interactions occurred between the side chains of Trp 251$^{6.48}$ and Tyr 281$^{7.39}$, and the 2-phenyl ring further stabilized the ligand conformation within the binding site (see Supporting Information figure S3 for a detailed representation of the binding site). The amide functionality of 2PhMLT was within close proximity to Met 107$^{3.32}$, with the methyl group interacting with the residue side chain. This region could also accommodate longer amide substituents,

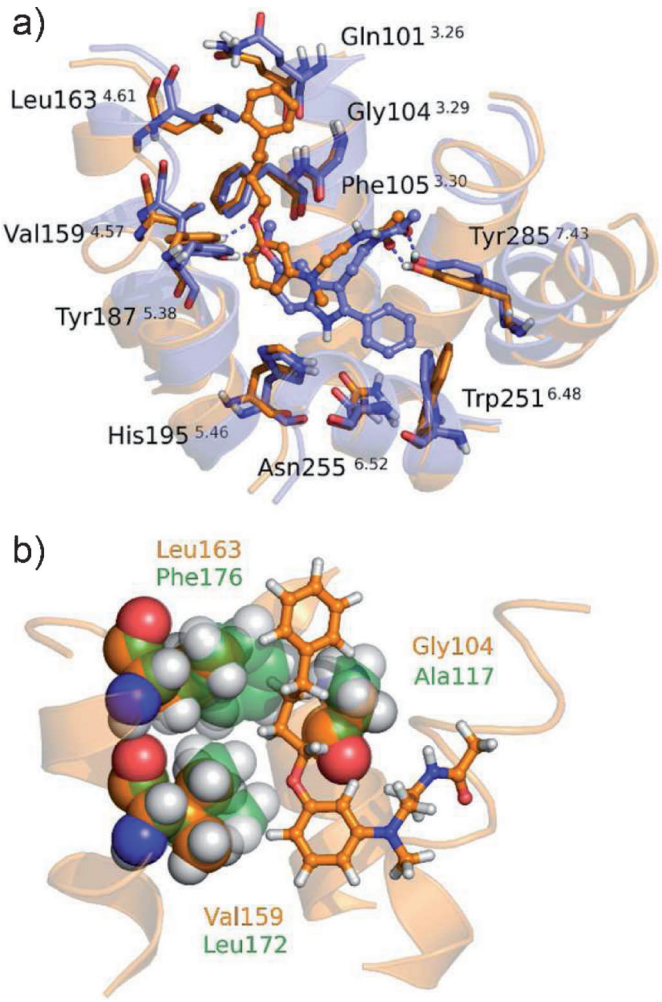

Figure 3. a) Energy-minimized structures of the MT_1 receptor in complex with 2PhMLT (purple) or **4a** (orange) after 50 ns MD simulation. Residues are depicted as sticks, whereas ligand molecules are shown in ball-and-stick representation. Hydrogen bonds are depicted as dashed blue lines. b) Close-up view of the MT_1 receptor–**4a** complex after MD simulation. The ligand molecule is represented as a ball-and-sticks model with orange carbons. Residues that differ between the MT_1 and MT_2 receptors are represented as orange (MT_1) and transparent green (MT_2) spheres.

 © 2012 Wiley-VCH Verlag GmbH & Co. KGaA, Weinheim

such as ethyl or propyl groups, consistent with SAR for different series of melatonin receptor agonists.[67]

To investigate the molecular basis of MT_1 selectivity, compound **4a** was docked into the refined MT_1 receptor model, obtained from the MD simulation of the MT_1–2PhMLT complex. IFD was applied to facilitate the accommodation of the bulky phenylbutyloxy chain of compound **4a**. In this case, the stability of the resulting MT_1 receptor–**4a** complex was also assessed through an MD simulation performed in a solvated lipid bilayer. The receptor structure was stable during the 50 ns MD simulation (Figure 2), as were the ligand–receptor interactions. As can be seen in Figure 3a, the lipophilic chain of compound **4a** leaned on the tip of TM3 and TM4, forming hydrophobic interactions with several amino acids such as Gln $101^{3.26}$, Gly $104^{3.29}$, Phe $105^{3.30}$, Val $159^{4.57}$, Leu $163^{4.61}$, and Leu 168, Gln 169, and Tyr 175 on extracellular loop 2 (ECL2). Interestingly, a sequence-based comparison of MT_1 and MT_2 receptors revealed that the MT_2 subtype has some bulkier residues in positions surrounding the phenylbutyloxy chain of compound **4a** (Figure 3b and Supporting Information figure S1). Indeed, Gly $104^{3.29}$, Val $159^{4.57}$, and Leu $163^{4.61}$ in the MT_1 receptor are replaced by Ala $117^{3.29}$, Leu $172^{4.57}$, and Phe $176^{4.61}$, respectively, in the MT_2 receptor. Based on this observation, it could be hypothesized that the bulkier amino acids in the MT_2 receptor hamper the accommodation of the phenylbutyloxy substituent of **4a**. Therefore, the different amino acid composition may provide a structural clue for the MT_1 selectivity observed among chemically different melatoninergic ligands characterized by the presence of bulky lipophilic chains in the position corresponding to position 5 of melatonin.

Conclusions

A series of *N*-{[(3-*O*-substituted)anilino]alkyl}acetamides were described as novel melatoninergic ligands, some of which were endowed with high binding affinity and good MT_1 subtype selectivity. Substituents in the C_3 aniline position differently affected binding affinity and intrinsic activity, depending on their nature. Introduction of a C_4- or C_6-methylenoxy substituent was tolerated by both receptor subtypes (**4k–l**), whereas an unfavorable effect was produced by the longer C_8-alkyloxy group (**4m**) or by conformationally constrained substituents (**4d–h**). In contrast, the non-selective MT_1/MT_2 ligand **2a** was successfully converted into the high affinity MT_1-selective ligand **4a** by replacing the ether methyl group with a phenylbutyl side chain. These results confirm the importance of replacing the methoxy group with a bulky substituent to achieve MT_1 selectivity and to help clarify the size and shape of the two MT_1 and MT_2 binding pockets.

Structural information derived from the 3D model of the MT_1 receptor in its active state was combined with SAR, pharmacophore, and mutagenesis data to propose a binding interaction scheme for agonists and a possible explanation for the MT_1 selectivity of compounds with a bulky lipophilic substituent on the ether oxygen. This receptor model, even with the intrinsic limitations due to the building procedure and the limited structural information available, could help to clarify the molecular basis of ligand binding and to propose structural modifications aimed at improving ligand potency and selectivity.

Experimental Section

Chemistry

General methods: Melting points were determined on a Büchi B-540 capillary melting point apparatus and are uncorrected. ^{1}H NMR spectra and ^{13}C NMR spectra were recorded on a Bruker Avance 200 spectrometer (^{1}H: 200 MHz; ^{13}C: 50 MHz) using $CDCl_3$ as solvent unless stated otherwise. Chemical shifts (δ scale) are reported in parts per million (ppm) relative to the central peak of the solvent. Coupling constants (*J* values) are given in Hz. EI-MS spectra (70 eV) were taken on a Fisons Trio 1000 instrument. Only molecular ions $[M]^+$ and base peaks are given. ESI-MS spectra were taken on a Waters Micromass Zq instrument. Only molecular ions [*M*+1] are given. Infrared spectra were obtained on a Nicolet Avatar 360 FT-IR spectrometer; absorbances are reported in $\tilde{\nu}$ (cm^{-1}). Elemental analyses for C, H, and N were performed on a Carlo Erba analyzer, and results are within 0.4% of calculated values. Column chromatography purifications were performed under flash conditions using Merck 230–400 mesh silica gel. Analytical thin layer chromatography (TLC) was carried out on Merck silica gel 60 F_{254} plates. The two radioligands, 2-[^{125}I]iodomelatonin (specific activity, 2000 Ci $mmol^{-1}$) and [^{35}S]GTPγS ([^{35}S]guanosine-5′-*O*-(3-thio-triphosphate); specific activity, 1000 Ci $mmol^{-1}$) were purchased from PerkinElmer. 2-(2-Bromoethyl)naphthalene was prepared according to a published method.[68]

General procedure for the synthesis of phenol derivatives 3a–c: A solution of BBr_3 (1 M in CH_2Cl_2, 20 mL, 20 mmol) diluted with dry CH_2Cl_2 (40 mL) was added dropwise to a solution of the suitable methoxy derivative **2a–c** (10 mmol) in dry CH_2Cl_2 (40 mL) at 0 °C, and the resulting mixture was stirred at room temperature for 18 h. The reaction mixture was neutralized with a 2 N aqueous solution of Na_2CO_3 and extracted with EtOAc. The organic phases were combined, dried (Na_2SO_4), and concentrated under reduced pressure to give a crude product that was purified by flash chromatography (silica gel; CH_2Cl_2/MeOH, 98:2).

***N*-{2-[(3-Hydroxyphenyl)methylamino]ethyl}acetamide (3a)**: White solid (1.58 g, 76%): mp: 74–76 °C (Et_2O/petroleum ether); ^{1}H NMR ($CDCl_3$): δ = 1.95 (s, 3H), 2.91 (s, 3H), 3.44 (m, 4H), 5.80 (br s, 1H), 6.29 (m, 3H), 6.71 (br s, 1H), 7.08 ppm (m, 1H); ^{13}C NMR ($CDCl_3$): δ = 171.2, 157.4, 150.9, 130.2, 104.6, 104.3, 99.7, 51.6, 38.3, 37.4, 23.2 ppm; MS (EI, 70 eV): *m/z* 208 $[M]^+$, 136 (100).[43]

***N*-{2-[(3-Hydroxyphenyl)methylamino]propyl}acetamide (3b)**: Oil (1.51 g, 68%): ^{1}H NMR ([D$_6$]DMSO/$CDCl_3$): δ = 1.51 (m, 2H), 1.65 (s, 3H), 2.90 (m, 2H), 3.06 ppm (m, 2H); ESI-MS (*m/z*): 223 [*M*+1]; ^{13}C NMR ($CDCl_3$): δ = 171.2, 157.4, 150.9, 130.2, 104.7, 104.3, 99.7, 51.4, 38.8, 37.6, 26.5, 23.3 ppm.

***N*-{2-[(3-Hydroxyphenyl)phenylamino]ethyl}acetamide (3c)**: See ref. [49] for details.

General procedure for the synthesis of *N*-[3-(substituted alkoxy)-anilinoalkyl]acetamides 4a–g, 4i–m, and 4o: Sodium hydride (80% in mineral oil, 0.017 g, 0.55 mmol) was added to a solution of the suitable phenol derivative **3a–c** (0.5 mmol) in dry DMF (2 mL) at −10 °C under nitrogen atmosphere. After stirring for 5 min, the suitable alkylating agent (0.8 mmol) was added to the reaction mixture, and stirring was continued for 8–16 h, allowing the mixture to rise to room temperature. The reaction mixture was poured

 © 2012 Wiley-VCH Verlag GmbH & Co. KGaA, Weinheim

These are not the final page numbers!

into water and extracted 3× with EtOAc. The organic phases were combined, washed once with brine, dried (Na_2SO_4), and concentrated to give the desired crude product, which was purified by silica gel flash chromatography using EtOAc as eluent.

***N*-(2-{Methyl-[3-(4-phenylbutoxy)phenyl]amino}ethyl)acetamide (4a)**: This compound was prepared according to the general procedure described above, starting from **3a** and 1-bromo-4-phenylbutane to yield a white solid (100 mg, 59%): mp: 57 °C (Et_2O/petroleum ether); ^{1}H NMR ($CDCl_3$): δ = 1.82 (m, 4H), 1.94 (s, 3H), 2.69 (m, 2H), 2.93 (s, 3H), 3.46 (m, 4H), 3.97 (t, 2H, J = 6.0), 5.60 (br s, 1H), 6.28–6.40 (m, 3H), 7.10–7.34 ppm (m, 6H); ^{13}C NMR ($CDCl_3$): δ = 170.4, 160.4, 150.9, 142.3, 130.0, 128.4, 128.3, 125.8, 105.5, 102.2, 99.7, 67.6, 51.8, 38.4, 37.4, 35.6, 29.0, 27.9, 23.3 ppm; IR (nujol): $\tilde{\nu}$ = 3309, 1638 cm^{-1}; MS (EI, 70 eV): m/z 340 $[M]^+$, 268 (100); Anal. calcd for $C_{21}H_{28}N_2O_2$: C 74.08, H 8.29, N 8.23, found: C 74.31, H 8.42, N 8.01.

***N*-(3-{Methyl-[3-(4-phenylbutoxy)phenyl]amino}propyl)acetamide (4b)**: This compound was prepared according to the general procedure described above, starting from **3b** and 1-bromo-4-phenylbutane to yield an oil (97 mg, 55% yield): ^{1}H NMR ($CDCl_3$): δ = 1.80 (m, 6H), 1.94 (s, 3H), 2.69 (m, 2H), 2.89 (s, 3H), 3.31 (m, 4H), 3.95 (t, 2H, J = 6.0), 5.53 (br s, 1H), 6.23–6.45 (m, 3H), 7.08–7.29 ppm (m, 6H); ^{13}C NMR ($CDCl_3$): δ = 170.1, 160.3, 150.6, 142.3, 130.0, 128.4, 128.3, 125.8, 105.6, 101.8, 99.8, 67.6, 50.5, 38.6, 37.8, 35.6, 29.0, 27.9, 27.0, 23.3 ppm; IR (neat): $\tilde{\nu}$ = 3289, 1650 cm^{-1}; ESI-MS (m/z): 355 $[M+1]$; Anal. calcd for $C_{22}H_{30}N_2O_2$: C 74.54, H 8.53, N 7.90, found: C 74.41, H 8.70, N 7.95.

***N*-(2-{Phenyl-[3-(4-phenylbutoxy)phenyl]amino}ethyl)acetamide (4c)**: This compound was prepared according to the general procedure described above, starting from **3c** and 1-bromo-4-phenylbutane to yield a white solid (90 mg, 45%): mp: 98–99 °C (Et_2O/petroleum ether); ^{1}H NMR ($CDCl_3$): δ = 1.80 (m, 4H), 1.92 (s, 3H), 2.68 (m, 2H), 3.50 (m, 2H), 3.90 (m, 4H), 5.61 (br s, 1H), 6.48–6.61 (m, 3H), 7.00–7.34 pm (m, 11H); ^{13}C NMR ($CDCl_3$): δ = 170.4, 160.2, 149.1, 147.6, 142.2, 130.0, 129.5, 128.4, 128.3, 125.8, 122.2, 121.8, 112.7, 107.0, 106.9, 67.7, 51.0, 37.9, 35.6, 28.9, 27.9, 23.2 ppm; IR (nujol): $\tilde{\nu}$ = 3322, 1647 cm^{-1}; ESI-MS (m/z): 403 $[M+1]$; Anal. calcd for $C_{26}H_{30}N_2O_2$: C 77.58, H 7.51, N 6.96, found: C 77.42, H 7.26, N 6.98.

***N*-(2-{[3-(2-Benzyloxyethoxy)phenyl]methylamino}ethyl)acetamide (4d)**: This compound was prepared according to the general procedure described above, starting from **3a** and benzyl 2-bromoethyl ether to yield an oil (104 mg, 61%): ^{1}H NMR ($CDCl_3$): δ = 1.93 (s, 3H), 2.92 (s, 3H), 3.44 (m, 4H), 3.83 (m, 2H), 4.15 (m, 2H), 4.64 (s, 2H), 5.58 (br s, 1H), 6.28–6.41 (m, 3H), 7.13 (m, 1H), 7.26–7.38 ppm (m, 5H); ^{13}C NMR ($CDCl_3$): δ = 170.4, 160.1, 150.8, 138.1, 130.0, 128.4, 127.8, 127.7, 105.8, 102.3, 99.9, 73.4, 68.6, 67.3, 51.8, 38.5, 37.3, 23.3 ppm; IR (neat): $\tilde{\nu}$ = 3297, 1655 cm^{-1}; ESI-MS (m/z): 343 $[M+1]$; Anal. calcd for $C_{20}H_{26}N_2O_3$: C 70.15, H 7.65, N 8.18, found: C 70.22, H 7.66, N 8.24.

***N*-(2-{[3-(Biphenyl-3-ylmethoxy)phenyl]methylamino}ethyl)acetamide (4e)**: This compound was prepared according to the general procedure described above, starting from **3a** and 3-phenylbenzyl bromide to yield a white solid (133 mg, 71%): mp: 80–81 °C (Et_2O/petroleum ether); ^{1}H NMR ($CDCl_3$): δ = 1.92 (s, 3H), 2.94 (s, 3H), 3.45 (m, 4H), 5.13 (s, 2H), 5.58 (br s, 1H), 6.39–6.43 (m, 3H), 7.16 (m, 1H), 7.30–7.59 ppm (m, 9H); ^{13}C NMR ($CDCl_3$): δ = 170.4, 160.1, 150.8, 141.6, 140.9, 137.8, 130.1, 129.0, 128.8, 127.4, 127.2, 126.8, 126.5, 126.4, 105.8, 102.5, 100.0, 70.0, 51.7, 38.5, 37.3, 23.2 ppm; IR (nujol): $\tilde{\nu}$ = 3280, 1635 cm^{-1}; MS (EI, 70 eV): m/z 374 $[M]^+$, 167 (100); Anal. calcd for $C_{24}H_{26}N_2O_2$: C 76.98, H 7.00, N 7.48, found: C 76.73, H 6.74, N 7.35.

***N*-(2-{[3-(Biphenyl-4-ylmethoxy)phenyl]methylamino}ethyl)acetamide (4f)**: This compound was prepared according to the general procedure described above, starting from **3a** and 4-phenylbenzyl bromide to yield a white solid (60 mg, 32%): mp: 122–123 °C (Et_2O); ^{1}H NMR ($CDCl_3$): δ = 1.94 (s, 3H), 2.95 (s, 3H), 3.46 (m, 4H), 5.11 (s, 2H), 5.57 (br s, 1H), 6.41–6.47 (m, 3H), 7.18 (m, 1H), 7.31–7.65 ppm (m, 9H); ^{13}C NMR ($CDCl_3$): δ = 170.4, 160.0, 150.9, 140.9, 140.8, 136.3, 130.0, 128.8, 128.1, 127.4, 127.3, 127.1, 105.8, 102.5, 100.0, 69.7, 51.7, 38.5, 37.3, 23.3 ppm; IR (nujol): $\tilde{\nu}$ = 3240, 1637 cm^{-1}; MS (EI, 70 eV): m/z 374 $[M]^+$, 167 (100); Anal. calcd for $C_{24}H_{26}N_2O_2$: C 76.98, H 7.00, N 7.48, found: C 77.12, H 7.29, N 7.59.

***N*-{2-[(3-Benzyloxyphenyl)methylamino]ethyl}acetamide (4g)**: This compound was prepared according to the general procedure described above, starting from **3a** and benzyl bromide to yield a white solid (56 mg, 38%): mp: 67–68 °C (Et_2O/petroleum ether); ^{1}H NMR ($CDCl_3$): δ = 1.93 (s, 3H), 2.93 (s, 3H), 3.45 (m, 4H), 5.07 (s, 2H), 5.58 (br s, 1H), 6.34–6.43 (m, 3H), 7.15 (m, 1H), 7.32–7.47 ppm (m, 5H); ^{13}C NMR ($CDCl_3$): δ = 170.4, 160.1, 150.8, 137.3, 130.0, 128.6, 127.9, 127.5, 105.8, 102.5, 100.0, 69.9, 51.7, 38.5, 37.3, 23.3 ppm; IR (nujol): $\tilde{\nu}$ = 3323, 1649 cm^{-1}; MS (EI, 70 eV): m/z 298 $[M]^+$, 91 (100); Anal. calcd for $C_{18}H_{22}N_2O_2$: C 72.46, H 7.43, N 9.39, found: C 72.49, H 7.38, N 9.09.

***N*-(2-{Methyl-[3-(6-phenylhexyloxy)phenyl]amino}ethyl)acetamide (4i)**: This compound was prepared according to the general procedure described above, starting from **3a** and 1-bromo-6-phenylhexane to yield a white solid (66 mg, 36%): mp: 58–59 °C (Et_2O/petroleum ether); ^{1}H NMR ($CDCl_3$): δ = 1.36–1.86 (m, 8H), 1.95 (s, 3H), 2.63 (m, 2H), 2.94 (s, 3H), 3.47 (m, 4H), 3.95 (t, 2H, J = 6.5), 5.60 (br s, 1H), 6.24–6.41 (m, 3H), 7.10–7.33 ppm (m, 6H); ^{13}C NMR ($CDCl_3$): δ = 170.4, 160.4, 150.9, 142.7, 130.0, 128.4, 128.2, 125.6, 105.5, 102.3, 99.7, 67.7, 51.8, 38.4, 37.4, 35.9, 31.4, 29.3, 29.0, 26.0, 23.3 ppm; IR (nujol): $\tilde{\nu}$ = 3312, 1652 cm^{-1}; MS (EI, 70 eV): m/z 368 $[M]^+$, 91 (100); Anal. calcd for $C_{23}H_{32}N_2O_2$: C 74.96, H 8.75, N 7.60, found: C 75.08, H 8.88, N 7.51.

***N*-(2-{Methyl-[3-(8-phenyloctyloxy)phenyl]amino}ethyl)acetamide (4j)**: This compound was prepared according to the general procedure described above, starting from **3a** and 1-bromo-8-phenyloctane to yield a white solid (105 mg, 53%): mp: 65–66 °C (Et_2O/petroleum ether); ^{1}H NMR ($CDCl_3$): δ = 1.28–1.84 (m, 12H), 1.94 (s, 3H), 2.61 (m, 2H), 2.93 (s, 3H), 3.46 (m, 4H), 3.94 (t, 2H, J = 6.5), 5.61 (br s, 1H), 6.28–6.40 (m, 3H), 7.10–7.32 ppm (m, 6H); ^{13}C NMR ($CDCl_3$): δ = 170.4, 160.4, 150.9, 142.9, 130.0, 128.4, 128.2, 125.6, 105.4, 102.3, 99.7, 67.8, 51.8, 38.4, 37.4, 36.0, 31.5, 29.44, 29.38, 29.34, 29.26, 26.1, 23.3 ppm; IR (nujol): $\tilde{\nu}$ = 3306, 1643 cm^{-1}; MS (EI, 70 eV): m/z 396 $[M]^+$, 91 (100); Anal. calcd for $C_{25}H_{36}N_2O_2$: C 75.72, H 9.15, N 7.06, found: C 75.34, H 9.49, N 7.22.

***N*-{2-[(3-Butoxyphenyl)methylamino]ethyl}acetamide (4k)**: This compound was prepared according to the general procedure described above, starting from **3a** and 1-bromobutane to yield a white solid (79 mg, 60%): mp: 68 °C (Et_2O/petroleum ether); ^{1}H NMR ($CDCl_3$): δ = 0.98 (t, 3H, J = 7.0), 1.50 (m, 2H), 1.77 (m, 2H), 1.94 (s, 3H), 2.94 (s, 3H), 3.46 (m, 4H), 3.96 (t, 2H, J = 6.5), 5.61 (br s, 1H), 6.29–6.41 (m, 3H), 7.14 ppm (m, 1H); ^{13}C NMR ($CDCl_3$): δ = 170.4, 160.4, 150.9, 130.0, 105.5, 102.3, 99.7, 67.5, 51.8, 38.4, 37.4, 31.4, 23.3, 19.3, 13.9 ppm; IR (nujol): $\tilde{\nu}$ = 3231, 1637 cm^{-1}; MS (EI, 70 eV): m/z 264 $[M]^+$, 192 (100); Anal. calcd for $C_{15}H_{24}N_2O_2$: C 68.15, H 9.15, N 10.60, found: C 68.23, H 9.30, N 10.69.

***N*-{2-[(3-Hexyloxyphenyl)methylamino]ethyl}acetamide (4l)**: This compound was prepared according to the general procedure described above, starting from **3a** and 1-bromohexane to yield a white solid (98 mg, 67%): mp: 56 °C (Et_2O/petroleum ether);

 © 2012 Wiley-VCH Verlag GmbH & Co. KGaA, Weinheim

^{1}H NMR ($CDCl_3$): $\delta=0.91$ (t, 3H, $J=6.5$), 1.27–1.62 (m, 6H), 1.77 (m, 2H), 1.94 (s, 3H), 2.94 (s, 3H), 3.46 (m, 4H), 3.96 (m, 2H), 5.64 (brs, 1H), 6.28–6.41 (m, 3H), 7.14 ppm (m, 1H); ^{13}C NMR ($CDCl_3$): $\delta=$ 170.4, 160.4, 150.9, 130.0, 105.4, 102.3, 99.7, 67.8, 51.8, 38.4, 37.4, 31.6, 29.4, 25.8, 23.2, 22.6, 14.05 ppm; IR (nujol): $\tilde{\nu}=3230$, 1630 cm^{-1}; MS (EI, 70 eV): *m/z* 292 $[M]^+$, 220 (100); Anal. calcd for $C_{17}H_{28}N_2O_2$: C 69.83, H 9.65, N 9.58, found: C 69.51, H 9.57, N 9.23.

***N*-{2-[Methyl-(3-octyloxyphenyl)amino]ethyl}acetamide (4m)**: This compound was prepared according to the general procedure above described starting from **3a** and 1-bromooctane. White solid (93 mg, 58%); mp 63–4 °C (Et_2O/petroleum ether); ^{1}H NMR ($CDCl_3$): $\delta=0.89$ (m, 3H), 1.25–1.49 (m, 10H), 1.77 (m, 2H), 1.94 (s, 3H), 2.94 (s, 3H), 3.46 (m, 4H), 3.94 (t, 2H, $J=6.5$), 5.63 (brs, 1H), 6.28–6.40 (m, 3H), 7.13 ppm (m, 1H); ^{13}C NMR ($CDCl_3$): $\delta=170.4$, 160.4, 150.9, 129.9, 105.4, 102.3, 99.7, 67.8, 51.8, 38.4, 37.4, 31.8, 29.4, 29.4, 29.3, 26.1, 23.3, 22.7, 14.1 ppm; IR (nujol): $\tilde{\nu}=3219$, 1610 cm^{-1}; MS (EI, 70 eV): *m/z* 320 $[M]^+$, 248 (100); Anal. calcd for $C_{19}H_{32}N_2O_2$: C 71.21, H 10.06, N 8.74, found: C 71.39, H 10.23, N 8.58.

{3-[(2-Acetylaminoethyl)methylamino]phenoxy}acetic acid methyl ester (4o): This compound was prepared according to the general procedure described above, starting from **3a** and methyl chloroacetate. The crude residue was purified by flash chromatography over silica gel, using EtOAc as an eluent to yield an amorphous solid (116 mg, 83%): ^{1}H NMR ($CDCl_3$): $\delta=1.94$ (s, 3H), 2.94 (s, 3H), 3.46 (m, 4H), 3.82 (s, 3H), 4.64 (s, 2H), 5.79 (brs, 1H), 6.22 (dd, 1H, $J=2.0$, 8.0), 6.37 (d, 1H, $J=2.0$), 6.42 (dd, 1H, $J=2.0$, 8.0), 7.14 ppm (t, 1H, $J=8.0$); ^{13}C NMR ($CDCl_3$): $\delta=170.5$, 169.7, 159.0, 150.8, 130.1, 106.5, 101.5, 99.9, 65.2, 52.2, 51.6, 38.5, 37.2, 23.2 ppm; ESI MS (*m/z*): 281 $[M+1]$.

***N*-(2-{Methyl-[3-(2-naphthalen-2-ylethoxy)phenyl]amino}ethyl)-acetamide (4h)**: K_2CO_3 (0.033 g, 0.24 mmol) was added to a solution of **3a** (0.05 g, 0.24 mmol) in CH_3CN (0.8 mL), and the resulting mixture was stirred and heated at 60 °C under nitrogen atmosphere for 20 min. 2-(2-Bromoethyl)naphthalene[68] was added to the reaction mixture, then heating and stirring was continued for 16 h. The reaction mixture was poured into water and extracted 3x with EtOAc. The organic phases were combined, washed once with brine, dried (Na_2SO_4), and concentrated to give the crude desired product, which was purified by silica gel flash chromatography with EtOAc as eluent to yield an oil (7 mg, 8%): ^{1}H NMR ($CDCl_3$): $\delta=1.93$ (s, 3H), 2.94 (s, 3H), 3.27 (t, 2H, $J=7.0$), 4.28 ppm (t, 2H, $J=7.0$); ^{13}C NMR ($CDCl_3$): $\delta=170.5$, 160.4, 150.9, 136.3 133.5, 132.4, 130.0, 128.3, 127.7, 127.6, 127.3, 126.9, 126.2, 125.7, 105.4, 102.2, 99.7, 67.7, 51.8, 38.4, 37.4, 35.6, 23.3 ppm; IR (neat): $\tilde{\nu}=3292$, 1658 cm^{-1}; MS (EI, 70 eV): *m/z* 362 $[M]^+$, 155 (100); Anal. calcd for $C_{23}H_{26}N_2O_2$: C 76.21, H 7.23, N, 7.73, found: C 76.02, H 7.15, N 7.69.

***N*-(2-{[3-(2-Hydroxyethoxy)phenyl]methylamino}ethyl)acetamide (4n)**: $LiAlH_4$ (0.085 g, 2.24 mmol) was added portionwise to a stirring solution of **4o** (0.330 g, 1.2 mmol) in dry THF (1 mL) under nitrogen atmosphere at 0 °C, and the resulting mixture was stirred at 0 °C for 1 h. Water was added dropwise to destroy the excess hydride, the resulting mixture was filtered over Celite, and the filtrate was concentrated in vacuo and partitioned between EtOAc and water. The combined organic phases were washed with brine, dried (Na_2SO_4), and concentrated to afford a crude residue, which was purified by flash chromatography over silica gel (EtOAc/MeOH, 95:5 as eluent) to yield a white solid (270 mg, 64%): mp: 86–87 °C (Et_2O/petroleum ether); ^{1}H NMR ($CDCl_3$): $\delta=1.94$ (s, 3H), 2.24 (t, 1H), 2.94 (s, 3H), 3.44 (m, 4H), 3.96 (m, 2H), 4.10 (m, 2H), 5.62 (brs, 1H), 6.28–6.40 (m, 3H), 7.14 ppm (m, 1H); ^{13}C NMR ($CDCl_3$): $\delta=$ 170.6, 160.0, 150.8, 130.1, 105.7, 102.5, 99.5, 69.0, 61.4, 51.7, 38.5, 37.3, 23.3 ppm; IR ($CDCl_3$): $\tilde{\nu}=3456$, 1668 cm^{-1}; ESI MS (*m/z*): 253 $[M+1]$; Anal. calcd for $C_{13}H_{20}N_2O_3$: C 61.88, H 7.99, N 11.10, found: C 61.98, H 8.11, N 11.36.

Pharmacology

Binding affinities were determined using 2-[^{125}I]iodomelatonin as the labeled ligand in competition experiments with cloned human MT_1 and MT_2 receptors expressed in NIH3T3 rat fibroblast cells. The characterization of NIH3T3 MT_1 and MT_2 cells was already described in detail.[69,70] Membranes were incubated for 90 min at 37 °C in binding buffer (50 mM Tris/HCl, pH 7.4). The final membrane concentration was 5–10 μg of protein per tube. The membrane protein level was determined in accordance with a previously reported method.[71] 2-[^{125}I]Iodomelatonin (100 pM) and different concentrations of the new compounds were incubated with the receptor preparation for 90 min at 37 °C. Nonspecific binding was assessed with 10 μM melatonin; IC_{50} values were determined by nonlinear fitting strategies with Prism (GraphPad SoftWare Inc., San Diego, CA). The pK_i values were calculated from the IC_{50} values in accordance with the Cheng–Prusoff equation.[53] The pK_i values are the mean of at least three independent determinations performed in duplicate.

To determine the functional activity of the new compounds at MT_1 and MT_2 receptor subtypes,[^{35}S]GTPγS binding assays in NIH3T3 cells expressing human-cloned MT_1 or MT_2 receptors were performed. The amount of bound [^{35}S]GTPγS is proportional to the level of the analogue-induced G protein activation and is related to the intrinsic activity of the compound under study. The detailed description and validation of this method were reported elsewhere.[69,72] Membranes (15–25 μg of protein, final incubation volume 100 μL) were incubated at 30 °C for 30 min in the presence and absence of melatonin analogues, in assay buffer consisting of [^{35}S]GTPγS (0.3–0.5 nM), GDP (50 μM), NaCl (100 mM), and $MgCl_2$ (3 mM). Nonspecific binding was defined using [^{35}S]GTPγS (10 μM). In cell lines expressing human MT_1 or MT_2 receptors, melatonin produced concentration-dependent stimulation of basal [^{35}S]GTPγS binding with a maximal stimulation above basal levels of 370% and 250% in MT_1 and MT_2 receptors, respectively. Basal stimulation is the amount of [^{35}S]GTPγS specifically bound in the absence of compounds and was taken as 100%. The maximal G protein activation was measured in each experiment using melatonin (100 nM). Compounds were added at three different concentrations (one concentration equivalent to 100 nM melatonin, a second one 10-fold smaller, and a third one 10-fold larger), and the percent stimulation above basal was determined. The equivalent concentration was estimated on the basis of the ratio of the affinity of the test compound to that of melatonin. It was assumed that, at the equivalent concentration, the test compound occupies the same number of receptors as 100 nM melatonin. All of the measurements were performed in triplicate. The relative intrinsic activity (IAr) values were obtained by dividing the maximum ligand-induced stimulation of [^{35}S]GTPγS binding by that of melatonin, as measured in the same experiment.

Molecular modeling

A number of X-ray structures have been obtained for GPCRs crystallized in their agonist-bound form, including rhodopsin, β_1 and β_2 adrenergic receptors, and A_{2A} adenosine receptor. However, despite the presence of co-crystallized agonists, only a limited

 © 2012 Wiley-VCH Verlag GmbH & Co. KGaA, Weinheim

These are not the final page numbers!

number of these GPCR structures shows the predicted pattern of structural rearrangements associated with the fully activated state.[73,74] In particular, the outward movement of the intracellular end of TM6, required to accommodate the C-terminus of the cognate G protein, was observed only in some agonist-bound forms of rhodopsin and the β_2 adrenergic receptor. The β_2 adrenergic receptor was selected as the template structure for homology modeling of the MT_1 receptor, sharing higher sequence identity with the TM regions (24%) than rhodopsin (22%). The amino acid sequence of the human MT_1 receptor and the X-ray crystal structure of the β_2 adrenergic receptor were retrieved from the Universal Protein Resource[75] (UniProt ID: P48039) and the Protein Data Bank (PDB code: 3P0G),[53] respectively. An initial sequence alignment was created with ClustalW2[76] and was subsequently refined, taking into account conserved sequence motifs among class A GPCRs.[58,77] In particular, highly conserved residues located on TM domains, as well as the conserved disulfide bridge connecting ECL2 and TM3, were considered during alignment refinement (Supporting Information figure S1).

Comparative modeling was carried out with Modeller 9.7,[78] and an ensemble of 30 MT_1 receptor models was initially generated. The 3D coordinates of residues 23 to 227 and 266 to 344 of the β_2 receptor were used as the template. For crystallization purposes, intracellular loop 3 of the β_2 receptor (residues 228–265) was replaced with the T4 lysozyme molecule, thus Modeller was used to rebuild the corresponding sequence of the MT_1 receptor (residues 216–230). The MT_1 receptor models begin at residue 17 and end at residue 314. Stereochemical quality assessment of the receptor models was performed with Procheck[79] and with the Protein Report tool implemented in Maestro 9.0.[80] Selection of the best model was based on the quality of geometrical parameters and on the Modeller objective function. The selected MT_1 receptor model was then processed through the Protein Preparation Wizard workflow[81] available in Maestro 9.0. Hydrogen atoms were added to the structure, and protonation states for ionizable side chains were chosen to be consistent with physiological pH. The overall hydrogen bonding network was optimized by adjusting the tautomerization states of histidine residues and by sampling the orientation of hydroxy and thiol groups, together with the side chain amides of asparagine and glutamine residues. Protein C- and N-termini were capped with neutral groups (acetyl and methylamino, respectively), and the all-hydrogen receptor model was then subjected to restrained minimization using the OPLS2001[82] force field to an RMSD of 0.5 Å. The Ramachandran plot for the final refined structure is reported in Supporting Information figure S2.

The structure of 2PhMLT was built with Maestro 9.0 and optimized to fit a pharmacophore model previously developed for nonselective melatoninergic agonists.[57] The acetylaminoethyl side chain of 2PhMLT showing the best fit is perpendicular to the indole ring in its extended conformation (torsion angles: C_{3a}-C_3-C_β-$C_\alpha \approx -90°$, C_3-C_β-C_α-N $\approx 180°$, C_β-C_α-N-CO $\approx 180°$, Figure 1). The 5-methoxy methyl group lies in the plane of the indole ring, directed toward position 4. The final ligand structure was minimized using the OPLS2005 force field[83] to a convergence threshold of 0.05 kJ mol^{-1} Å^{-1}. An IFD protocol was applied to account for both ligand and receptor flexibility during ligand docking.[55] An initial softened-potential docking run was performed, applying van der Waals radii scaling of 0.7 and 0.5 on protein and ligand non-polar atoms, respectively. Amino acids hampering accommodation of 2PhMLT into the binding crevice (Val 111$^{3.36}$, Trp 251$^{6.48}$, and Tyr 281$^{7.39}$) were temporarily mutated to alanines. Energy grids generated for the initial softened-potential docking were centered on Met 107$^{3.32}$ and His 195$^{5.46}$, setting the enclosing and bounding boxes to default dimensions. 2PhMLT was rigidly docked into the MT_1 receptor binding site to retain the postulated bioactive conformation. Ligand docking was performed in the standard precision mode, collecting fifty poses for subsequent analysis. Resulting ligand–receptor complexes were then submitted to a protein structure refinement stage; once amino acid side chains that had previously been removed were re-introduced, residues within a shell of 6 Å around any ligand pose were refined by a side chain conformational search, followed by energy minimization of the residues and the ligand molecule. In the final docking stage, 2PhMLT was rigidly re-docked into each receptor structure produced in the previous refinement step, applying default Glide settings. The IFD score, accounting for protein–ligand interaction energy and the total energy of the system, was used to rank the final ligand–receptor complexes. Mutagenesis studies of the MT_1 receptor[59,60] suggested a role of His 195$^{5.46}$ in the stabilization of the 5-methoxy group of melatonin (see main text). Therefore, the best ranked ligand–receptor complex with the 5-methoxy substituent within proximity of His 195$^{5.46}$ was selected for further analysis. The MT_1 receptor–2PhMLT complex was minimized using the Amber force field[84] implemented in MacroModel 9.7[85] and by applying the Polak–Ribiere conjugate gradient method to a convergence threshold of 0.05 kJ mol^{-1} Å^{-1}; the ligand and residues within 8 Å proximity of the ligand were free to move, while all other atoms were fixed. The resulting structure was then prepared for MD simulation using Desmond version 2.2.6.2.3:[86,87] accordingly, the energy-minimized ligand–receptor complex was embedded in a POPC lipid bilayer by aligning the receptor to the 3P0G crystal structure deposited into the Orientations of Protein in Membranes (OPM) database,[88] with at least 20 Å between the protein and its closest periodic image. The protein membrane system was solvated by approximately 10700 T3P water molecules in a simulation box of 77 Å × 74 Å × 99 Å. The Amber99SB[89] force field was used to model the protein, while ligand and lipids were parameterized using GAFF.[90] Partial atomic charges of 2PhMLT were computed by the Antechamber module[91] of AmberTools 10 at the AM1-BCC level. The system was relaxed using a modified version of a membrane relaxation protocol implemented in the Desmond package. The equilibration phase was followed by a 50 ns long MD simulation performed in the NPT ensemble at 310 K and 1 atm using the Langevin coupling scheme.[92] All bond lengths to hydrogen atoms were constrained using M-SHAKE.[93] Short-range electrostatic interactions were cut off at 9 Å, whereas long-range electrostatic interactions were computed using the Smooth Particle Mesh Ewald method.[94] A RESPA integrator[95] was used with a time-step of 2 fs, and long-range electrostatics were computed every 6 fs.

Compound **4a** was optimized with the OPLS2005 force field to a convergence threshold of 0.05 kJ mol^{-1} Å^{-1}. An IFD protocol was then applied to dock **4a** into the MT_1 structure obtained from the energy-minimized final snapshot of the MD simulation performed on the MT_1–2PhMLT complex. Glide scoring grids for subsequent docking calculations were centered on the 2PhMLT pose obtained at the end of the MD simulation. Compound **4a** was docked flexibly, imposing the formation of a hydrogen bond between the Tyr 187$^{5.38}$ hydroxy group and the phenolic oxygen of the ligand, and between the Tyr 285$^{7.43}$ hydroxy group and the amide oxygen, to produce the same pattern of polar interactions as 2-PhMLT. To favor the accommodation of the bulky phenylbutyloxy chain of compound **4a**, Leu 163$^{4.61}$ and Gln 181, located on ECL2, were temporarily mutated to alanines. The MT_1–**4a** complex, having the best IFD score and with the amide side chain conformation of **4a** consistent with the pharmacophore model for nonselective mela-

 © 2012 Wiley-VCH Verlag GmbH & Co. KGaA, Weinheim

tonin receptor agonists, was chosen. Ligand atoms and residues within a sphere of 8 Å around the ligand were submitted to an energy minimization procedure, applying the Amber force field, to a convergence threshold of 0.05 $kJ\,mol^{-1}\,Å^{-1}$. The final MT_1 receptor–**4a** complex was re-introduced in the pre-equilibrated lipid bilayer obtained from the MD simulation performed on the MT_1–2PhMLT complex. The resulting system was then submitted to a 50 ns MD simulation applying the protocol previously described.

Acknowledgements

The authors thank Dr. Jeff Wereszczynski (University of California, San Diego, USA) for providing the GAFF templates for Desmond. This work was supported by Universities of Parma, Milano and Urbino "Carlo Bo".

Keywords: melatonin · molecular modeling · MT_1 selectivity · structure–activity relationships

[1] J. Barrenetxe, P. Delagrange, J. A. Martinez, *J. Physiol. Biochem.* **2004**, *60*, 61 – 72.
[2] S. R. Pandi-Perumal, I. Trakht, V. Srinivasan, D. W. Spence, G. J. Maestroni, N. Zisapel, D. P. Cardinali, *Prog. Neurobiol.* **2008**, *85*, 335 – 353.
[3] J. Arendt, *J. Biol. Rhythms* **2005**, *20*, 291 – 303.
[4] V. Srinivasan, M. Smits, W. Spence, A. D. Lowe, L. Kayumov, S. R. Pandi-Perumal, B. Parry, D. P. Cardinali, *World J. Biol. Psychiatry* **2006**, *7*, 138 – 151.
[5] M. D. Maldonado, R. J. Reiter, M. A. Perez-San-Gregorio, *Hum. Psychopharmacol.* **2009**, *24*, 391 – 400.
[6] G. J. Maestroni, *Expert Opin. Invest. Drugs* **2001**, *10*, 467 – 476.
[7] F. Simko, O. Pechanova, *J. Pineal Res.* **2009**, *47*, 127 – 133.
[8] M. Ambriz-Tututi, H. I. Rocha-González, S. L. Cruz, V. Granados-Soto, *Life Sci.* **2009**, *84*, 489 – 498.
[9] J. C. Mayo, R. M. Sainz, D. X. Tan, R. Hardeland, J. Leon, C. Rodriguez, R. J. Reiter, *J. Neuroimmunol.* **2005**, *165*, 139 – 149.
[10] R. Hardeland, *Endocrine* **2005**, *27*, 119 – 130.
[11] R. Hardeland, *Molecules* **2009**, *14*, 5054 – 5102.
[12] D. E. Blask, L. A. Sauer, R. T. Dauchy, *Curr. Top. Med. Chem.* **2002**, *2*, 113 – 132.
[13] E. Mills, P. Wu, D. Seely, G. Guyatt, *J. Pineal Res.* **2005**, *39*, 360 – 366.
[14] N. Bouatia-Naji, A. Bonnefond, C. Cavalcanti-Proença, T. Sparsø, J. Holmkvist, M. Marchand, J. Delplanque, S. Lobbens, G. Rocheleau, E. Durand, F. De Graeve, J. C. Chèvre, K. Borch-Johnsen, A. L. Hartikainen, A. Ruokonen, J. Tichet, M. Marre, J. Weill, B. Heude, M. Tauber et al., *Nat. Genet.* **2009**, *41*, 89 – 94.
[15] V. Lyssenko, C. L. Nagorny, M. R. Erdos, N. Wierup, A. Jonsson, P. Spégel, M. Bugliani, R. Saxena, M. Fex, N. Pulizzi, B. Isomaa, T. Tuomi, P. Nilsson, J. Kuusisto, J. Tuomilehto, B. Boehnke, D. Altshuler, F. Sundler, J. G. Eriksson, A. U. Jackson et al., *Nat. Genet.* **2009**, *41*, 82 – 88.
[16] A. G. Wade, I. Ford, G. Crawford, A. D. McMahon, T. Nir, M. Laudon, N. Zisapel, *Curr. Med. Res. Opin.* **2007**, *23*, 2597 – 2605.
[17] M. Miyamoto, *CNS Neurosci. Ther.* **2009**, *15*, 32 – 51.
[18] C. de Bodinat, B. Guardiola-Lemaitre, E. Mocaër, P. Renard, C. Muñoz, M. J. Millan, *Nat. Rev. Drug Discovery* **2010**, *9*, 628 – 642.
[19] D. P. Cardinali, V. Srinivasan, A. Brzezinski, G. M. Brown, *J. Pineal Res.* **2012**, *52*, 365 – 375.
[20] G. Spadoni, A. Bedini, S. Rivara, M. Mor, *CNS Neurosci. Ther.* **2011**, *17*, 733 – 741.
[21] M. L. Dubocovich, P. Delagrange, D. N. Krause, D. Sugden, D. P. Cardinali, J. Olcese, *Pharmacol. Rev.* **2010**, *62*, 343 – 380.
[22] R. Jockers, P. Maurice, J. A. Boutin, P. Delagrange, *Br. J. Pharmacol.* **2008**, *154*, 1182 – 1195.
[23] S. M. Reppart, D. R. Weaver, C. Godson, *Trends Pharmacol. Sci.* **1996**, *17*, 100 – 102.
[24] O. Nosjean, M. Ferro, F. Cogé, P. Beauverger, J. M. Henlin, F. Lefoulon, J. L. Fauchere, P. Delagrange, E. Canet, J. A. Boutin, *J. Biol. Chem.* **2000**, *275*, 31311 – 31317.
[25] C. Ekmekcioglu, *Biomed. Pharmacother.* **2006**, *60*, 97 – 108.
[26] M. L. Dubocovich, M. Markowska, *Endocrine* **2005**, *27*, 101 – 110.
[27] X. Jin, C. von Gall, R. L. Pieschl, V. K. Gribkoff, J. H. Stehle, S. M. Reppert, D. R. Weaver, *Mol. Cell. Biol.* **2003**, *23*, 1054 – 1060.
[28] C. von Gall, M. L. Garabette, C. A. Kell, S. Frenzel, F. Dehghani, P. M. Schumm-Draeger, D. R. Weaver, H. W. Korf, M. H. Hastings, J. H. Stehle, *Nat. Neurosci.* **2002**, *5*, 234 – 238.
[29] K. Baba, N. Pozdeyev, F. Mazzoni, S. Contreras-Alcantara, C. Liu, M. Kasamatsu, T. Martinez-Merlos, E. Strettoi, P. M. Iuvone, G. Tosini, *Proc. Natl. Acad. Sci. USA* **2009**, *106*, 15043 – 15048.
[30] C. Ersahin, M. I. Masana, M. L. Dubocovich, *Eur. J. Pharmacol.* **2002**, *439*, 71 – 172.
[31] M. I. Masana, S. Doolen, C. Ersahin, W. M. Al-Ghoul, S. P. Duckles, M. L. Dubocovich, D. N. Krause, *J. Pharmacol. Exp. Ther.* **2002**, *302*, 1295 – 1302.
[32] D. L. Drazen, R. J. Nelson, *Neuroendocrinology* **2001**, *74*, 178 – 184.
[33] M. L. Dubocovich, M. I. Masana, S. Iacob, D. M. Sauri, *Naunyn Schmiedebergs Arch. Pharmacol.* **1997**, *355*, 365 – 375.
[34] M. L. Dubocovich, K. Yun, W. M. Al-Ghoul, S. Benloucif, M. I. Masana, *FASEB J.* **1998**, *12*, 1211 – 1220.
[35] R. Ochoa-Sanchez, S. Comai, B. Lacoste, F. R. Bambico, S. Dominguez-Lopez, G. Spadoni, S. Rivara, A. Bedini, D. Angeloni, F. Fraschini, M. Mor, G. Tarzia, L. Descarries, G. Gobbi, *J. Neurosci.* **2011**, *31*, 18439 – 18452.
[36] D. P. Zlotos, *Arch. Pharm.* **2005**, *338*, 229 – 247.
[37] M. Mor, S. Rivara, D. Pala, A. Bedini, G. Spadoni, G. Tarzia, *Expert Opin. Ther. Pat.* **2010**, *20*, 1059 – 1077.
[38] D. P. Zlotos, *Curr. Med. Chem.* **2012**, *19*, 3532 – 3549.
[39] C. Descamps-Francois, S. Yous, P. Chavatte, V. Audinot, A. Bonnaud, J. A. Boutin, P. Delagrange, C. Bennejean, P. Renard, D. J. Lesieur, *J. Med. Chem.* **2003**, *46*, 1127 – 1129.
[40] C. Mésangeau, B. Pérès, C. Descamps-Francois, P. Chavatte, V. Audinot, S. Coumailleau, J. A. Boutin, P. Delagrange, C. Bennejean, P. Renard, D.-H. Caignard, P. Berthelot, S. Yous, *Bioorg. Med. Chem.* **2010**, *18*, 3426 – 3436.
[41] B. Di Giacomo, A. Bedini, G. Spadoni, G. Tarzia, F. Fraschini, M. Pannacci, V. Lucini, *Bioorg. Med. Chem.* **2007**, *15*, 4643 – 4650.
[42] C. Larraya, J. Guillard, P. Renard, V. Audinot, J. A. Boutin, P. Delagrange, C. Bennejean, M.-C. Viaud-Massuard, *Eur. J. Med. Chem.* **2004**, *39*, 515 – 526.
[43] G. Spadoni, A. Bedini, P. Orlando, S. Lucarini, G. Tarzia, M. Mor, S. Rivara, V. Lucini, M. Pannacci, F. Scaglione, *Bioorg. Med. Chem.* **2011**, *19*, 4910 – 4916.
[44] a) L. Q. Sun, J. Chen, M. Bruce, J. A. Deskus, J. R. Epperson, K. Takaki, G. Johnson, L. Iben, C. D. Mahle, E. Ryan, C. Xu, *Bioorg. Med. Chem. Lett.* **2004**, *14*, 3799 – 3802; b) L. Q. Sun, J. Chen, K. Takaki, G. Johnson, L. Iben, C. D. Mahle, E. Ryan, C. Xu, *Bioorg. Med. Chem. Lett.* **2004**, *14*, 1197 – 1200; c) L. Q. Sun, K. Takaki, J. Chen, L. Iben, J. O. Knipe, L. Pajor, C. D. Mahle, E. Ryan, C. Xu, *Bioorg. Med. Chem. Lett.* **2004**, *14*, 5157 – 5160.
[45] V. Audinot, F. Mailliet, C. Lahaye-Brasseur, A. Bonnaud, A. Le Gall, C. Amossé, S. Dromaint, M. Rodriguez, N. Nagel, J. P. Galizzi, B. Malpaux, G. Guillaumet, D. Lesieur, F. Lefoulon, P. Renard, P. Delagrange, J. A. Boutin, *Naunyn Schmiedebergs Arch. Pharmacol.* **2003**, *367*, 553 – 561.
[46] C. Markl, W. P. Clafshenkel, M. I. Attia, S. Sethi, P. A. Witt-Enderby, D. P. Zlotos, *Arch. Pharm.* **2011**, *344*, 666 – 674.
[47] F. Lezoualc'h, R. Jockers, I. Berque-Bestel, *Curr. Pharm. Des.* **2009**, *15*, 719 – 729.
[48] S. Rivara, A. Lodola, M. Mor, A. Bedini, G. Spadoni, V. Lucini, M. Pannacci, F. Fraschini, F. Scaglione, R. O. Sanchez, G. Gobbi, G. Tarzia, *J. Med. Chem.* **2007**, *50*, 6618 – 6626.
[49] S. Rivara, F. Vacondio, A. Fioni, C. Silva, C. Carmi, M. Mor, V. Lucini, M. Pannacci, A. Caronno, F. Scaglione, G. Gobbi, G. Spadoni, A. Bedini, P. Orlando, S. Lucarini, G. Tarzia, *ChemMedChem* **2009**, *4*, 1746 – 1755.
[50] S. Rivara, S. Lorenzi, M. Mor, P. V. Plazzi, G. Spadoni, A. Bedini, G. Tarzia, *J. Med. Chem.* **2005**, *48*, 4049 – 4060.
[51] D. Sugden, H. Pickering, T. Mui-Teck, P. J. Garratt, *Biol. Cell* **1997**, *89*, 531 – 537.

 © 2012 Wiley-VCH Verlag GmbH & Co. KGaA, Weinheim

[52] R. Nonno, V. Lucini, G. Spadoni, M. Pannacci, A. Croce, D. Esposti, C. Balsamini, G. Tarzia, F. Fraschini, B. M. Stankov, *J. Pineal Res.* **2000**, *29*, 234 – 240.
[53] C. Yung-Chi, W. H. Prusoff, *Biochem. Pharmacol.* **1973**, *22*, 3099 – 3108.
[54] S. G. F. Rasmussen, B. T. DeVree, Y. Zou, A. C. Kruse, K. Y. Chung, T. S. Kobilka, F. S. Thian, P. S. Chae, E. Pardon, D. Calinski, J. M. Mathiesen, S. T. A. Shah, J. A. Lyons, M. Caffrey, S. H. Gellman, J. Steyaert, G. Skiniotis, W. I. Weis, R. K. Sunahara, B. K. Kobilka, *Nature* **2011**, *477*, 549 – 555.
[55] a) Schrödinger Suite 2011 Induced Fit Docking protocol; b) Glide version 5.7, Schrödinger, LLC, New York, NY, **2011**; c) Prime version 3.0, Schrödinger, LLC, New York, NY, **2011**.
[56] G. Spadoni, B. Stankov, A. Duranti, G. Biella, V. Lucini, A. Salvatori, F. Fraschini, *J. Med. Chem.* **1993**, *36*, 4069 – 4074.
[57] S. Rivara, G. Diamantini, B. Di Giacomo, D. Lamba, G. Gatti, V. Lucini, M. Pannacci, M. Mor, G. Spadoni, G. Tarzia, *Bioorg. Med. Chem.* **2006**, *14*, 3383 – 3391.
[58] J. A. Ballesteros, H. Weinstein in *Methods in Neurosciences*, (Eds.: S. C. Sealfon, P. M. Conn), Elsevier, **1995**, pp. 366 – 428.
[59] S. Conway, S. J. Canning, P. Barrett, B. Guardiola-Lemaitre, P. Delagrange, P. J. Morgan, *Biochem. Biophys. Res. Commun.* **1997**, *239*, 418 – 423.
[60] T. Kokkola, M. A. Watson, J. White, S. Dowell, S. M. Foord, J. T. Laitinen, *Biochem. Biophys. Res. Commun.* **1998**, *249*, 531 – 536.
[61] M. J. Gerdin, F. Mseeh, M. L. Dubocovich, *Biochem. Pharmacol.* **2003**, *66*, 315 – 320.
[62] P. Mazna, V. Obsilova, I. Jelinkova, A. Balik, K. Berka, Z. Sovova, R. Ettrich, P. Svoboda, T. Obsil, J. Teisinger, *J. Neurochem.* **2004**, *91*, 836 – 842.
[63] V.-P. Jaakola, M. T. Griffith, M. A. Hanson, V. Cherezov, E. Y. T. Chien, J. R. Lane, A. P. IJzerman, R. C. Stevens, *Science* **2008**, *322*, 1211 – 1217.
[64] V.-P. Jaakola, J. R. Lane, J. Y. Lin, V. Katritch, A. P. IJzerman, R. C. Stevens, *J. Biol. Chem.* **2010**, *285*, 13032 – 13044.
[65] M. Conner, S. R. Hawtin, J. Simms, D. Wootten, Z. Lawson, A. C. Conner, R. A. Parslow, M. Wheatley, *J. Biol. Chem.* **2007**, *282*, 17405 – 17412.
[66] A. Cavalli, F. Fanelli, C. Taddei, P. G. De Benedetti, S. Cotecchia, *FEBS Lett.* **1996**, *399*, 9 – 13.
[67] S. Rivara, M. Mor, A. Bedini, G. Spadoni, G. Tarzia, *Curr. Top. Med. Chem.* **2008**, *8*, 954 – 968.
[68] G. J. Ellames, J. M. Herbert, *J. Labelled Compd. Radiopharm.* **2010**, *53*, 801 – 803.
[69] R. Nonno, V. Lucini, M. Pannacci, C. Mazzucchelli, D. Angeloni, F. Fraschini, B. M. Stankov, *Br. J. Pharmacol.* **1998**, *124*, 485 – 492.
[70] R. Nonno, M. Pannacci, V. Lucini, D. Angeloni, F. Fraschini, B. M. Stankov, *Br. J. Pharmacol.* **1999**, *127*, 1288 – 1294.
[71] M. M. Bradford, *Anal. Biochem.* **1976**, *72*, 248 – 254.
[72] G. Spadoni, C. Balsamini, A. Bedini, G. Diamantini, B. Di Giacomo, A. Tontini, G. Tarzia, M. Mor, P. V. Plazzi, S. Rivara, R. Nonno, M. Pannacci, V. Lucini, F. Fraschini, B. M. Stankov, *J. Med. Chem.* **1998**, *41*, 3624 – 3634.
[73] X. Deupi, J. Standfuss, *Curr. Opin. Struct. Biol.* **2011**, *21*, 541 – 551.
[74] G. Lebon, T. Warne, C. G. Tate, *Curr. Opin. Struct. Biol.* **2012**, DOI: 10.1016/j.sbi.2012.03.007.
[75] The UniProt Consortium, *Nucleic Acids Res.* **2011**, *40*, D71 – D75.
[76] J. D. Thompson, D. G. Higgins, T. J. Gibson, *Nucleic Acids Res.* **1994**, *22*, 4673 – 4680.
[77] T. Mirzadegan, G. Benko, S. Filipek, K. Palczewski, *Biochemistry* **2003**, *42*, 4310 – 4310.
[78] A. Sali, T. L. Blundell, *J. Mol. Biol.* **1993**, *234*, 779 – 815.
[79] R. A. Laskowski, M. W. MacArthur, D. S. Moss, J. M. Thornton, *J. Appl. Crystallogr.* **1993**, *26*, 283 – 291.
[80] Maestro, version 9.0, Schrödinger, LLC, New York, NY, **2009**.
[81] a) Schrödinger Suite 2009 Protein Preparation Wizard; b) Epik version 2.0, Schrödinger LLC, New York, NY, **2009**; c) Impact version 5.5, Schrödinger LLC, New York, NY, **2009**; d) Prime version 2.1, Schrödinger, LLC, New York, NY, **2009**.
[82] W. L. Jorgensen, D. S. Maxwell, J. Tirado-Rives, *J. Am. Chem. Soc.* **1996**, *118*, 11225 – 11236.
[83] G. A. Kaminski, R. A. Friesner, J. Tirado-Rives, W. L. Jorgensen, *J. Phys. Chem. B* **2001**, *105*, 6474 – 6487.
[84] S. J. Weiner, P. A. Kollman, D. A. Case, U. C. Singh, C. Ghio, G. Alagona, S. Profeta, P. Weiner, *J. Am. Chem. Soc.* **1984**, *106*, 765 – 784.
[85] MacroModel, version 9.7, Schrödinger, LLC, New York, NY, **2009**.
[86] a) Desmond Molecular Dynamics System, version 2.2, D. E. Shaw Research, New York, NY, **2009**; b) Maestro-Desmond Interoperability Tools, version 2.2, Schrödinger, New York, NY, **2009**.
[87] E. C. K. J. Bowers, H. Xu, R. O. Dror, M. P. Eastwood, B. A. Gregersen, J. L. Klepeis, I. Kolossvary, M. A. Moraes, F. D. Scaerdoti, J. K. Salmon, Y. Shan, D. E. Shaw, Proceedings of the 2006 ACM/IEEE Conference on Supercomputing (SC06), **2006**.
[88] M. A. Lomize, A. L. Lomize, I. D. Pogozheva, H. I. Mosberg, *Bioinformatics* **2006**, *22*, 623 – 625.
[89] V. Hornak, R. Abel, A. Okur, B. Strockbine, A. Roitberg, C. Simmerling, *Proteins Struct. Funct. Bioinf.* **2006**, *65*, 712 – 725.
[90] J. Wang, R. M. Wolf, J. W. Caldwell, P. A. Kollman, D. A. Case, *J. Comput. Chem.* **2004**, *25*, 1157 – 1174.
[91] J. Wang, W. Wang, P. A. Kollman, D. A. Case, *J. Mol. Graphics Modell.* **2006**, *25*, 247 – 260.
[92] S. E. Feller, Y. Zhang, R. W. Pastor, B. R. Brooks, *J. Chem. Phys.* **1995**, *103*, 4613 – 4621.
[93] R. A. Lippert, K. J. Bowers, R. O. Dror, M. P. Eastwood, B. A. Gregersen, J. L. Klepeis, I. Kolossvary, D. E. Shaw, *J. Chem. Phys.* **2007**, *126*, 046101.
[94] U. Essmann, L. Perera, M. L. Berkowitz, T. Darden, H. Lee, L. G. Pedersen, *J. Chem. Phys.* **1995**, *103*, 8577 – 8593.
[95] M. Tuckerman, B. J. Berne, G. J. Martyna, *J. Chem. Phys.* **1992**, *97*, 1990 – 2001.

Received: June 19, 2012
Revised: July 27, 2012
Published online on ■■ ■■, 0000

 © 2012 Wiley-VCH Verlag GmbH & Co. KGaA, Weinheim

*S. Rivara, D. Pala, A. Lodola, M. Mor, V. Lucini, S. Dugnani, F. Scaglione, A. Bedini, S. Lucarini, G. Tarzia, G. Spadoni**

■■ – ■■

MT_1-Selective Melatonin Receptor Ligands: Synthesis, Pharmacological Evaluation, and Molecular Dynamics Investigation of *N*-{[(3-*O*-Substituted)anilino]alkyl}amides

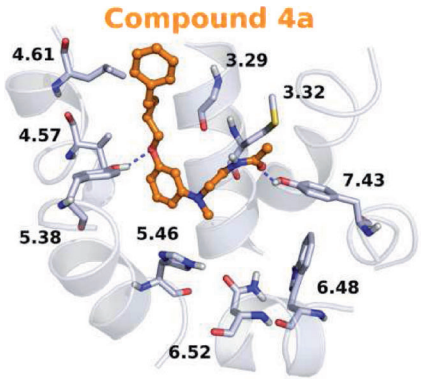

Focusing on selectivity: A new series of MT_1-selective agonists was synthesized by modulating the versatile *N*-anilinoethylamide scaffold through introduction of lipophilic (aryl)alkyl substituents on the ether oxygen atom. A combination of molecular modeling studies and ligand-based information provided hypotheses for ligand–receptor interactions and for MT_1 subtype selectivity.

 © 2012 Wiley-VCH Verlag GmbH & Co. KGaA, Weinheim